SUPPLEMENTARY DISCUSSION

Treatment of NESGFP^{u} expressing HEK293 cells with Lc resulted in a dosedependent increase in the abundance of high molecular weight Ub-immunoreactive protein with a concomitant decrease in the abundance of ubiquitylated histone 2A (Fig. S1, left). This well-documented[29] stereotypical response to proteasome inhibition is due to a shift of the distribution of cellular Ub from one dominated by mono-Ub to one enriched in polyubiquitin chain conjugates — a conclusion supported by the anti-Ub immunoreactivity of the high-molecular weight smear, by its disappearance upon treatment with the deubiquitylating enzyme Usp2cc, and by its efficient binding to hP2UBA (Fig. S1, right).

The hP2UBA binding reaction was allowed to reach equilibrium (Fig. S2a) as confirmed by the demonstration that the absolute amount of each captured peptide or isopeptide species increased linearly with increasing amounts of cell lysate over a 20-fold range (Fig. S2b). Moreover, the ratio of each polyubiquitin species to total Ub remained constant over this range of input loads (Fig. S2c), demonstrating that, under the conditions of excess of Ub binding capacity, the different Ub species in the lysate do not compete with one another for binding to hP2UBA. Finally, the total amount of Ub captured by hP2UBA, determined by mass spectrometry, correlates remarkably well with the amount of total Ub measured by an enzyme-linked immunosorbent assay (ELISA)[30] Fig. S2d). Thus, despite a higher affinity of hP2UBA for polyubiquitin compared to mono-Ub[31], the affinity captured material provides a faithful representation of the relative abundance of the different Ub species present in cell homogenates. The observed increase in UbK48 levels in HEK293 cells exposed to Lc is a post-transcriptional event, as Ub mRNA transcripts, assessed by quantitative rtPCR, did not significantly increase during the course of the experiment, despite the activation of the two stress-inducible polyubiquitin genes, *UbB* and *UbC* (Fig. S3).

29. Mimnaugh, E. G., Chen, H. Y., Davie, J. R., Celis, J. E. & Neckers, L. Rapid deubiquitination of nucleosomal histones in human tumor cells caused by proteasome inhibitors and stress response inducers: effects on replication, transcription, translation, and the cellular stress response. *Biochemistry* **36**, 14418-29 (1997).

30. Ryu, K. Y., Baker, R. T. & Kopito, R. R. Ubiquitin-specific protease 2 as a tool for quantification of total ubiquitin levels in biological specimens. *Anal Biochem* **353**, 153-5 (2006).

31. Raasi, S., Varadan, R., Fushman, D. & Pickart, C. M. Diverse polyubiquitin interaction properties of ubiquitin-associated domains. *Nat Struct Mol Biol* **12**, 708-14 (2005).

Figure S1

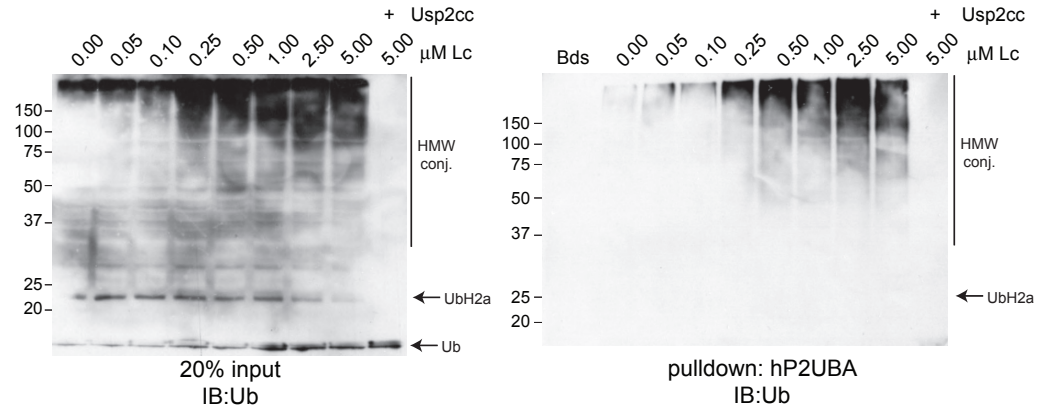

Figure S1: Proteasome inhibitor treatment shifts cellular Ub pools to high molecular weight conjugates. Ub immunoblot analysis of lysates (left) or hP2UBA-captured protein (right) from NESGFPu expressing HEK293 cells treated with the indicated concentrations of Lc for 8 hr. An aliquot of the cell lysate from Lc-treated cells was digested with Usp2cc as noted.

Figure S2

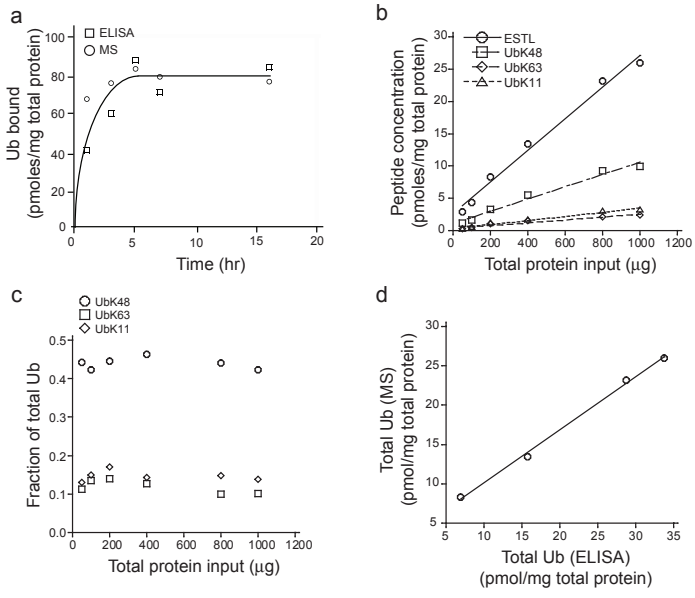

Figure S2 : hP2UBA-captured Ub species represent an unbiased sampling of cellular Ub pools. a, Timecourse of hP2UBA capture. HEK293 cell lysates were incubated with hP2UBA resin for the indicated times. Bound Ub species were eluted and analyzed by ELISA (squares) or mass spectrometry (MS; circles). **b**, Captured Ub isopeptides and peptides increase linearly with increasing protein input. Increasing amounts of cell lysate from 10µM MG132 treated HEK293 cells were incubated with a fixed amount of hP2UBA. hP2UBA bound material was eluted from the resin,digested with trypsin and then analyzed by LC-ESI-TOF mass spectrometry. The peptide concentrations of ESTL (circles), UbK48 (squares), UbK63 (diamonds), and UbK11 (triangles) were measured using spiked standards as in Fig. 1. Shown are the linear least squares fits for each data set; corresponding R values are all greater than 0.97. **c**, The fraction of total Ub captured as polyubiquitin chains is independent of protein input amount. The ratio of UbK48 (circles), UbK63 (squares), and UbK11 (diamonds) to total Ub (UbK63+ESTL) over increasing concentrations of input cell lysate. **d**, Linear correlation between ELISA and mass spectrometry measurements on total hP2UBA-captured Ub. Increasing concentrations of cell lysate from HEK293 cells treated with MG132 (10µM, 14 hr) were incubated with a fixed amount of hP2UBA. hP2UBA bound material was eluted from the matrix and the total Ub concentration was measured by ELISA, or quantified by LC-ESI-TOF mass spectrometry using spiked peptide standards. Total Ub from the mass spectrometry analysis was estimated from the sum of ESTL and UbK63 peptide concentrations. Solid line is the linear least squares fit; R = 0.9986.

Figure S3

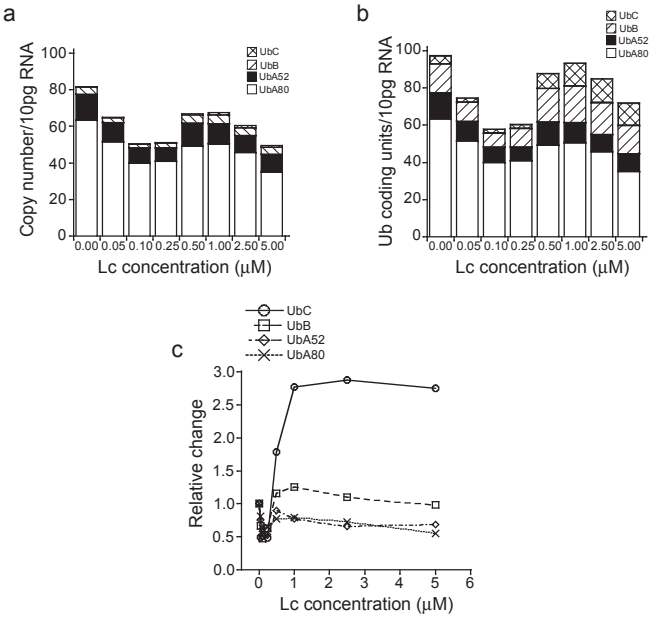

Figure S3 : Ub mRNA levels do not increase with increasing Lc concentrations. **a**, Total RNA was extracted from mouse N2a cells treated with increasing amounts of clasto-lactacystin β-lactone (Lc) for 8 hours. The total amount of transcripts from UbA52 (filled bar), UbA80 (open bar), UbB (hatched bar), and UbC (double hatched bar) genes was quantified at each Lc concentration using RT-PCR and normalized to 18S rRNA. **b**, To obtain an estimation of the total amount of Ub that could arise from the combined transcript levels the total Ub coding units per transcript was calculated as the normalized copy number multiplied by the Ub coding units from each gene. The sum of the bars represents the total amount of Ub coding units at each Lc concentration; UbA52 (filled bar) 1 coding unit, UbA80 (open bar) 1 coding unit, UbB (hatched bar) 4 coding units, UbC (double hatched bar) 9 coding units. **c**, The relative change in transcript levels of the four Ub genes over increasing Lc concentration. UbA52 (diamonds), UbA80 (crosses), UbB (squares), and UbC (circles) (n=3)

Figure S4

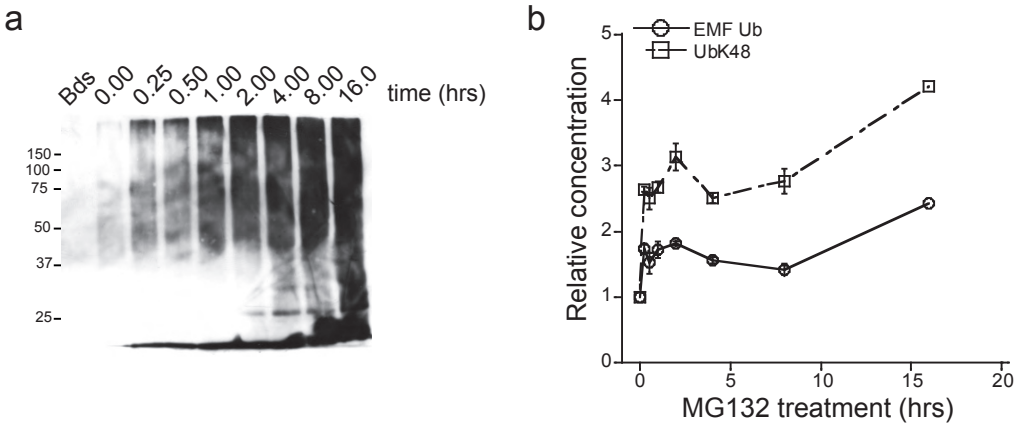

Figure S4: UbK48 isopeptide ion intensity increases with time of MG132 treatment. a, Mouse N2a cells were treated with 10μM MG132 over time. At the indicated times cell lysates were created and polyubiquitylated material was captured by hP2UBA resin. A sample of the 16 hour MG132 treated sample was mixed with control beads (bds). **b**, Material was eluted from the hP2UBA resin, digested with trypsin and then analyzed by LC-ESI-TOF mass spectrometry. Peptide concentrations were measured using spiked standards as in Fig. 1. The relative change in UbK48 isopeptide (circles, solid line), or EMF-Ub (square, dashed line) from hP2UBA isolated material is plotted over increasing time of MG132 treatment (n=3).

Figure S5

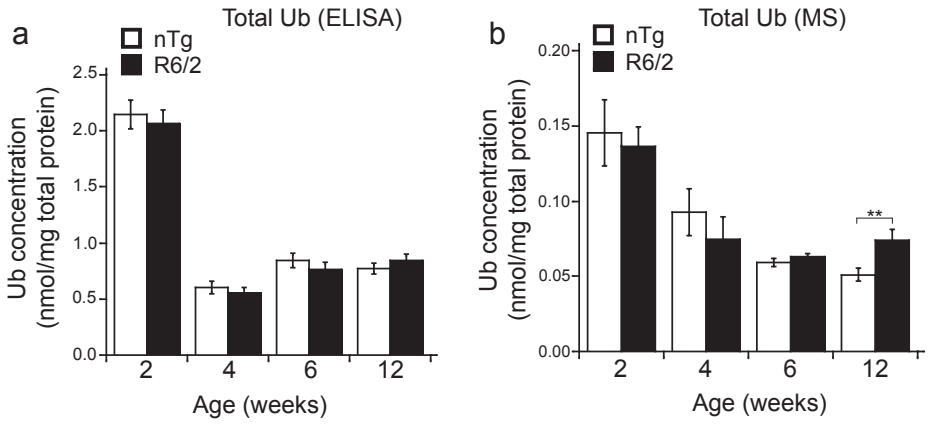

Figure S5: Total Ub levels are unaffected by the presence of the Htt transgene in R6/2 mice. a,b, Total Ub concentration, measured by ELISA in unfractionated cortical homogenates (**a**) or by mass spectrometry from hP2UBA-captured material from the same homogenates (**b**) of brains from R6/2 mice (filled bars) and non-transgenic littermates (nTg; open bars) at the indicated ages (n=12 for each genotype). All data are mean ± SEM. ** = $p \leq 0.01$ as determined by Student's t-test.

Figure S6

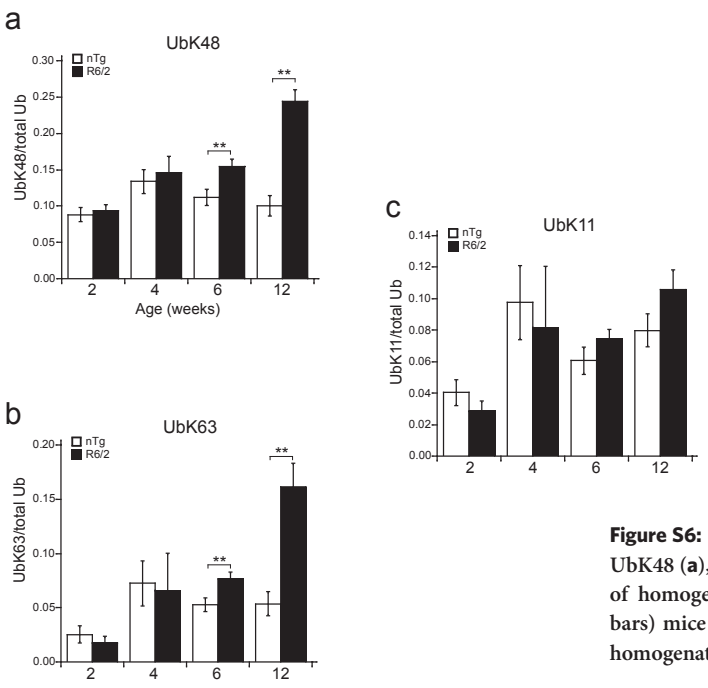

Figure S6: Increased fraction of total Ub in polyubiquitin chains in R6/2 mice. UbK48 (**a**), UbK63 (**b**), and UbK11 (**c**) isopeptide levels in hP2UBA pulldowns of homogenates of cortex from nontransgenic (open bars), or R6/2 (filled bars) mice divided by total Ub concentration as measured by ELISA in same homogenates prior to hP2UBA fractionation.

Figure S7

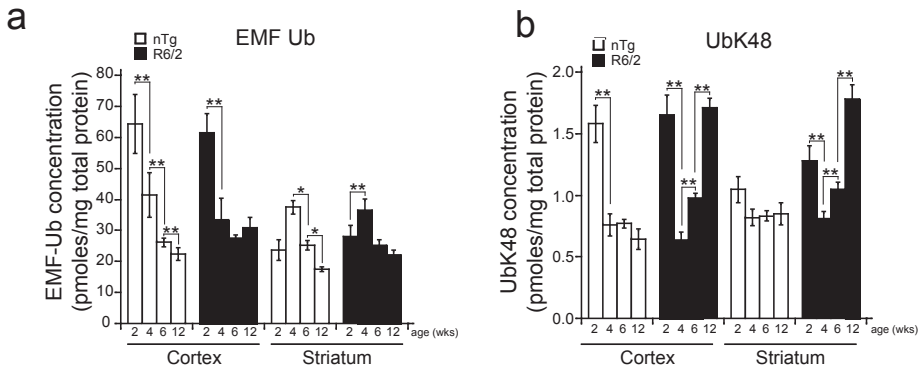

Figure S7: Age-dependent decrease in EMF-Ub and K48Ub levels mice. EMF-Ub (**a**) and UbK48 (**b**) concentrations in hP2UBA pulldowns from homogenates of cortex and striatum of R6/2 (filled bars) and non-transgenic littermate (nTg; open bars) mice (n=12 for each genotype).

Table. S1 : Human brain specimens used in this study.

AGE	GENDER	PMI	DIAGNOSIS	REGION
6	M	2:23	NDAR	BA4
15	M	2:30	NDAR	BA4
83	M	4:40	PD	BA4
79	M	3:28	PD	BA4
69	M	9:20	PD	BA4
81	M	N/A	NDAR	BA9
68	M	2:09	NDAR	BA9
55	M	6:05	NDAR	BA9
64	F	7:50	NDAR	BA9
57	M	N/A	NDAR	BA9
57	F	2:24	NDAR	BA9
74	M	4:15	NDAR	BA9
87	M	5:10	NDAR	BA9
74	F	18:45	NDAR	BA9
39	M	3:50	HD, grade 4	BA4
17	F	N/A	JHD	BA4
41	M	2:40	HD, grade 4	BA4
41	F	2:45	HD, grade 3	BA4
24	M	5:35	HD, grade 3	BA4
65	F	6:35	HD, grade 3	GP
61	M	17:05	HD, grade 3	CAP
47	M	2:20	HD, grade 3	CAP
72	M	15:30	HD, grade 2	GP
60	M	5:25	HD, grade 3	GP
56	F	0:40	HD, grade 4	CAP
36	M	0:40	HD, grade 4	BA4
61	F	16:20	HD, grade 3	CAP
72	M	11:55	HD, grade 3	CAP

Abbreviations used: BA, Braak area; CAP, caudate, accumbens, putamen; GP, globus pallidus, putamen; JHD, juvenile HD; N/A, data not available; NDAR, no diagnostic abnormality recognized; PD, Parkinson's disease; PMI, post-mortem interval calculated from the reported time of death to the time patient was brought to cold room